Journal of Cereal Science **27** (1998) 191–197

Research Note

Moisture Distribution in a Mature Soft Wheat Grain by Three-Dimensional Magnetic Resonance Imaging‡

H. P. Song*, S. R. Delwiche* and M. J. Line†

** Agricultural Engineers, Instrumentation and Sensing Laboratory, Beltsville Agricultural Research Center, Agricultural Research Service, USDA, Beltsville, Maryland, U.S.A.*

† Electrical Engineer, Environmental Chemistry Laboratory, Beltsville Agricultural Research Center, Agricultural Research Service, USDA, Beltsville, Maryland, U.S.A.

Received 11 November 1996

ABSTRACT

Moisture-tempering is typically performed prior to first break in wheat milling operations to enhance separation of bran, germ, and endosperm. To improve the milling performance and to increase yield, a better knowledge of moisture distribution and migration in individual wheat grains during tempering is essential. The research described herein was conducted to demonstrate the non-destructive measurement of the three-dimensional (3D) distribution of moisture in a single wheat grain.

A 3D magnetic resonance imaging (MRI) technique was adapted for the probing of single wheat grains at storage moistures (*c.* 12% wet basis). The technique is demonstrated in this report on one grain. A 3D projection reconstruction (3DPR) technique was used to acquire high resolution proton density images. The spatial resolution of the images was $94 \times 94 \times 94\ \mu m^3$. The 3D proton density images were related to the 3D moisture distribution in the wheat grain. At 12% moisture content, the moisture distribution in the starchy endosperm of the wheat was not uniform. The variation of the moisture distribution was from 7·3% to 16·4% wb.

Keywords: wheat, magnetic resonance imaging, moisture, single grain.

INTRODUCTION

The distribution and migration of moisture in wheat grains during storage are important for controlling milling, dough handling, and baking operations. Traditional studies of moisture within a grain have involved its physical dissection. Such a procedure is disruptive to the location of the moisture and does not permit the examination of diffusion within the same grain. Thus, an *in situ* procedure for moisture measurement is desirable. Acoustic measurement[1] and microwave heating[2] were investigated as indirect indications of moisture content. Magnetic resonance (MR) spectroscopy has also been used for non-destructive determination of average moisture content in corn, wheat, barley, and grain sorghum from 15 to 40% [wet basis (wb)] moisture[3], in whole grain wheat and barley[4] and in wheat in the 8 to 15% wb

ABBREVIATIONS USED: 3D = three-dimensional; PR = projection reconstruction; MRI = magnetic resonance imaging; w.b. = wet basis; FT = Fourier transform; T_2 = spin-spin relaxation time; T_E = echo time; RF = radio frequency; 2D = two-dimensional; T_1 = spin-lattice relaxation time.

Corresponding author: S. R. Delwiche. E-mail: sdelwiche@asrr.arsusda.gov

‡*Mention of company or trade names is for purpose of description only and does not imply endorsement by the U.S. Department of Agriculture.*

0733–5210/98/020191 + 07 $25.00/0/jc970163

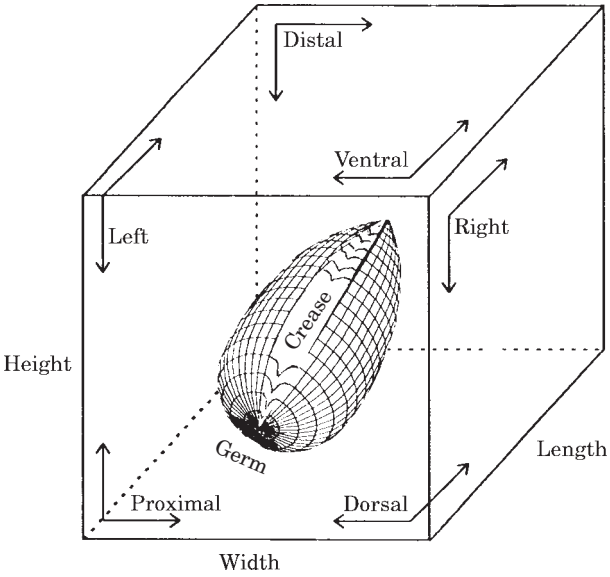

Figure 1 Three-dimensional layout of a wheat grain. Planes (i.e. faces of surrounding cube) are labelled according to word associated with each orthogonal axis pair. Grain is situated with the germ nearest to the proximal plane and the crease nearest to the ventral plane.

range[5]. However, none of these methods permit the investigation of how moisture is distributed within the seed.

Two-dimensional (2D) magnetic resonance imaging (MRI) has been applied to single grain research during the past 10 years[6,7]. More recently, three-dimensional (3D) MRI at sub-millimeter resolution has been used to measure moisture distribution in single grains. Three common methods are used for capture and processing of 3D MR images: (in order of increasing complexity and sensitivity[8]) (1) multislice, (2) three-dimensional Fourier transform (3DFT), and (3) three-dimensional projection reconstruction (3DPR). Briefly, the multislice method collects imaging data from multiple two-dimensional slices in sequence. Once slice 1 is excited and data collection from this slice is completed, slice 2 is excited and so on until the repetition time for image contrast has elapsed, whereupon the process begins anew with slice 1[9]. In the 3DFT method, the 3D Fourier transform of the images is recorded directly. This method

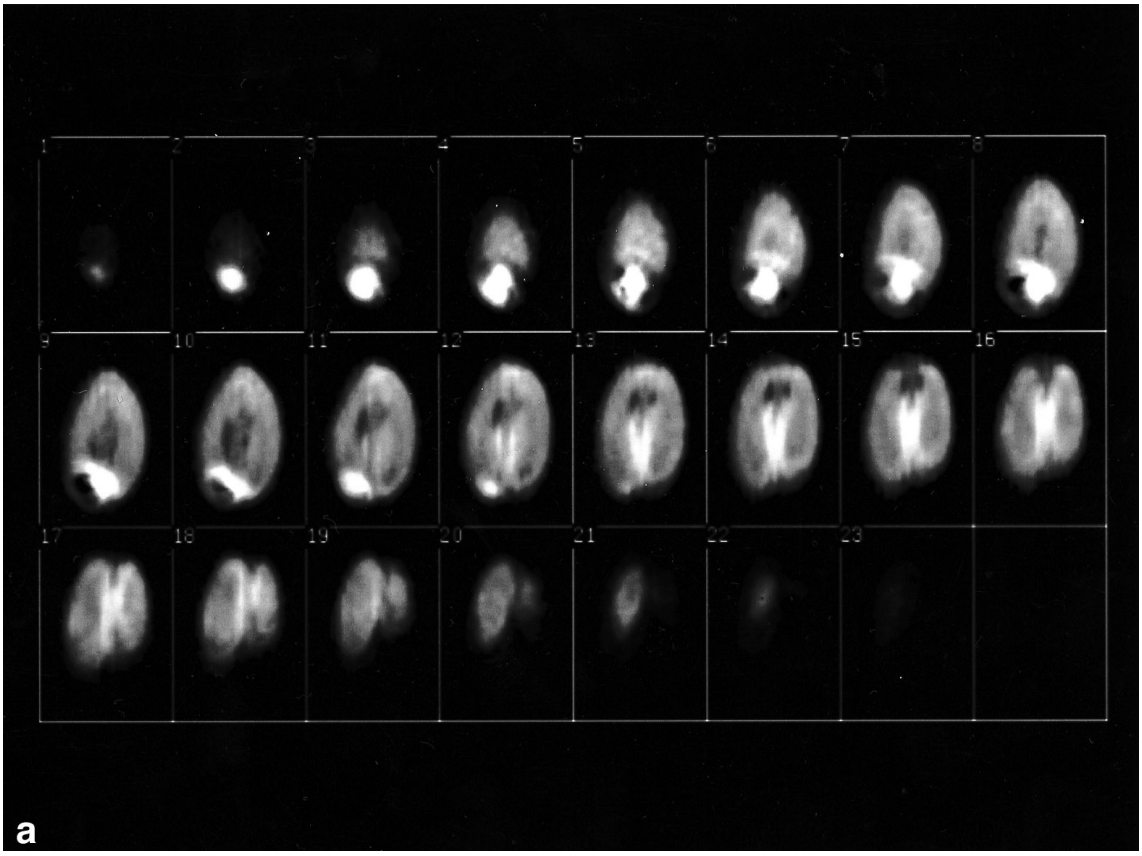

Figure 2 The 3D proton density of a wheat grain displayed as a series of 2D MR image slices (numbered within each set from upper left to lower right): (a) Dorsal-to-front view set (slices 1–23), (b) right-to-left view set (slices 1–21), and (c) distal-to-proximal view set (slices 1–35).—*contd opposite*

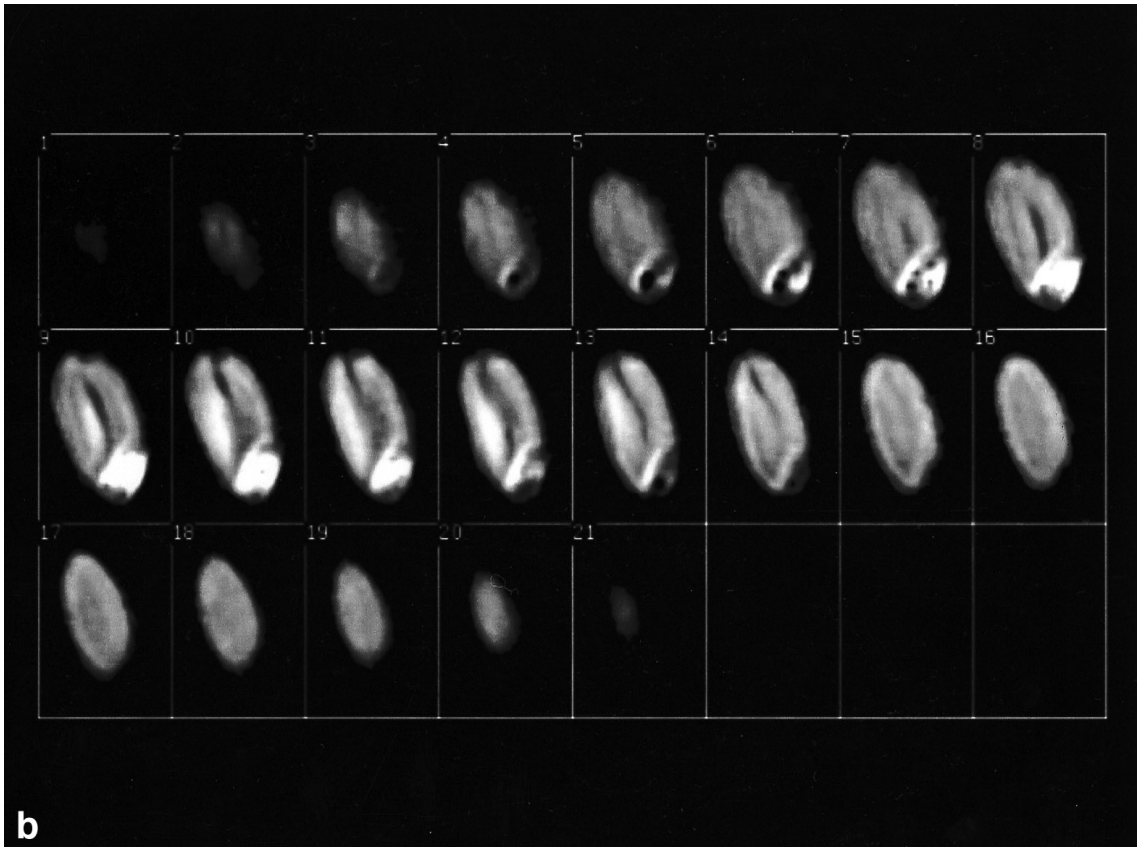
1
2
3
4
5
6
7
8
9
10
11
12
13
14
15
16
17
18
19
20
21
b

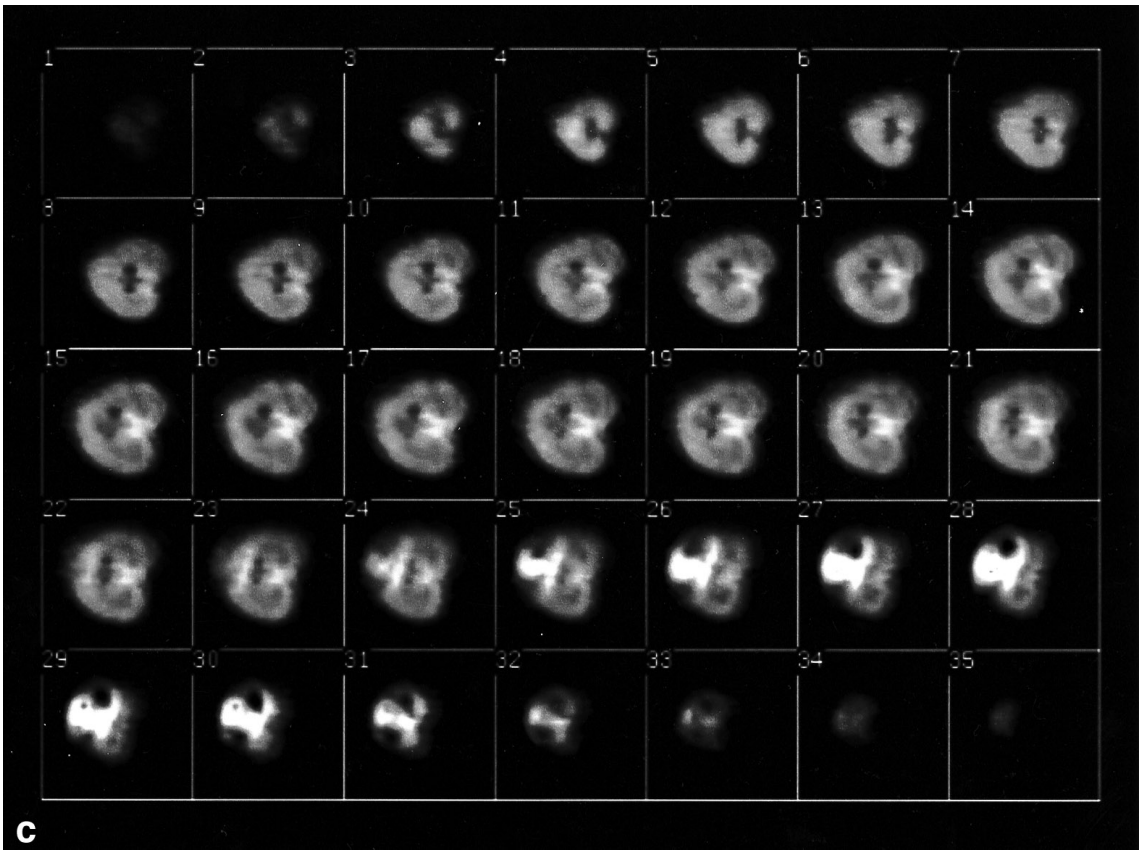
1
2
3
4
5
6
7
8
9
10
11
12
13
14
15
16
17
18
19
20
21
22
23
24
25
26
27
28
29
30
31
32
33
34
35
c

utilises a sequence of switched gradients and has the advantage that reconstruction of the image can be performed by straightforward Fourier transformation. A drawback is the time requirement for switching between three orthogonal gradients during an imaging cycle. Only partial signal energy is acquired during the observation period because of the spin–spin relaxation time decay of the transverse magnetisation when the other two gradients are present. With the 3DPR method, the image is reconstructed from each of a sufficient number of projections of the magnetic resonance signal intensity from the sample[10–14]. Each profile is back-projected in a direction orthogonal to the applied magnetic field gradient from which it was produced. The projection is then Fourier transformed and multiplied by a filter function. This product is then inversely transformed to give one filtered projection. A final image is formed by back-projecting the filtered projection onto the image plane with interpolation[15]. One of the advantages of this method is that all volume elements contribute to each projection. Also within each imaging cycle, three gradients are always on without switching, hence there is no loss in transverse magnetisation for gradient switching. The sensitivity of the 3DPR technique is invariably higher than that of 3DFT. The disadvantages of the 3DPR method are, a higher sensitivity to magnetic field inhomogeneity and a requirement of large computational power for image reconstruction.

In a study on the cracking in soybeans during drying (initial moisture contents of 25–35% wb), both multislice and 3DFT methods were sufficient for monitoring moisture loss, though the latter method provided better resolution[16]. Three-dimensional moisture distribution and structural changes in individual corn grains during drying (36 to 20% wb) have also been measured by 3DFT[17–19]. Recently, a 3DFT pulse sequence was used to obtain 3D proton images (78 μm × 62 μm × 62 μm spatial resolution) of single wheat grains at *c.* 12% wb[20]. The signal intensity of the images, however, was too weak in the endosperm to reveal fine detail on the distribution of moisture.

The objective of this study was to refine the 3DPR MRI technique to measure the distribution of moisture in single wheat grains at storage moisture levels, and to demonstrate this technique with one grain as an example. Because of its importance to milling performance, the moisture distribution in the endosperm was of specific interest.

EXPERIMENTAL

Mature soft red winter wheat grains were stored at 0–5°C for approximately 15 months after harvest. One to two weeks prior to MRI analysis the grains were allowed to reach moisture equilibrium within the laboratory (*c.* 20–23°C, 50% RH). Average moisture content of the samples was approximately 12% wb. For the example presented in this report, a medium-size sound grain was selected for imaging at room temperature.

A Bruker MSL-400 (Bruker Instruments, Inc., Billerica, MA, U.S.A.) spectrometer (9·4 Tesla) with a gradient coil was used to acquire images of individual wheat grains. A custom-made 5-mm diameter solenoid radio frequency (RF) probe was built to specifically fit a single wheat grain. The axial length of the RF coil was 15 mm, with the wheat grain (typically 6-mm long) positioned in the centre of the RF coil during imaging. The gradient amplifier switching time was 1 ms, a major limiting factor for better quality images of solid-state samples such as low-moisture wheat. Images were reconstructed and processed on a Sun SPARCstation™ computer with an image processing software package ("Viewit," National Centre for Supercomputing Applications, Urbana, IL, U.S.A.) and custom-written software.

A 3DPR technique with a Hahn spin-echo pulse sequence[21] was applied to acquire microscopic 3D images of wheat grains. This is the most common pulse sequence used in MRI. The signal intensity, S, from a volume element (voxel), assuming a rectangular pulse profile, is

$$S = \mathcal{N}(H)\,[1 - 2e^{-(T_R - T_E/2)/T_1} + e^{-T_R/T_1}]\,[e^{-T_E/T_2}]\,[e^{-bD}] \quad (1)$$

where $\mathcal{N}(H)$ is the proton density, T_E is echo time (the time between the 90° RF pulse and the formation of the spin echo), and T_R is the sequence repetition time (the time to perform the total sequence), T_1 is spin–lattice relaxation time and T_2 is the spin–spin relaxation time of the voxel. D is the water diffusion coefficient and b is a constant. Because D is a very small value, the diffusion factor $\exp(-bD)$ is almost unity. By varying the two user-selected delay times, T_E and T_R, this sequence can be used to highlight spin-density $\mathcal{N}(H)$, T_1, or T_2 effects. For most biological materials, T_E is usually much smaller than T_R, therefore

$$S = \mathcal{N}(H)\,[1 - e^{-T_R/T_1}]\,[e^{-T_E/T_2}] \quad (2)$$

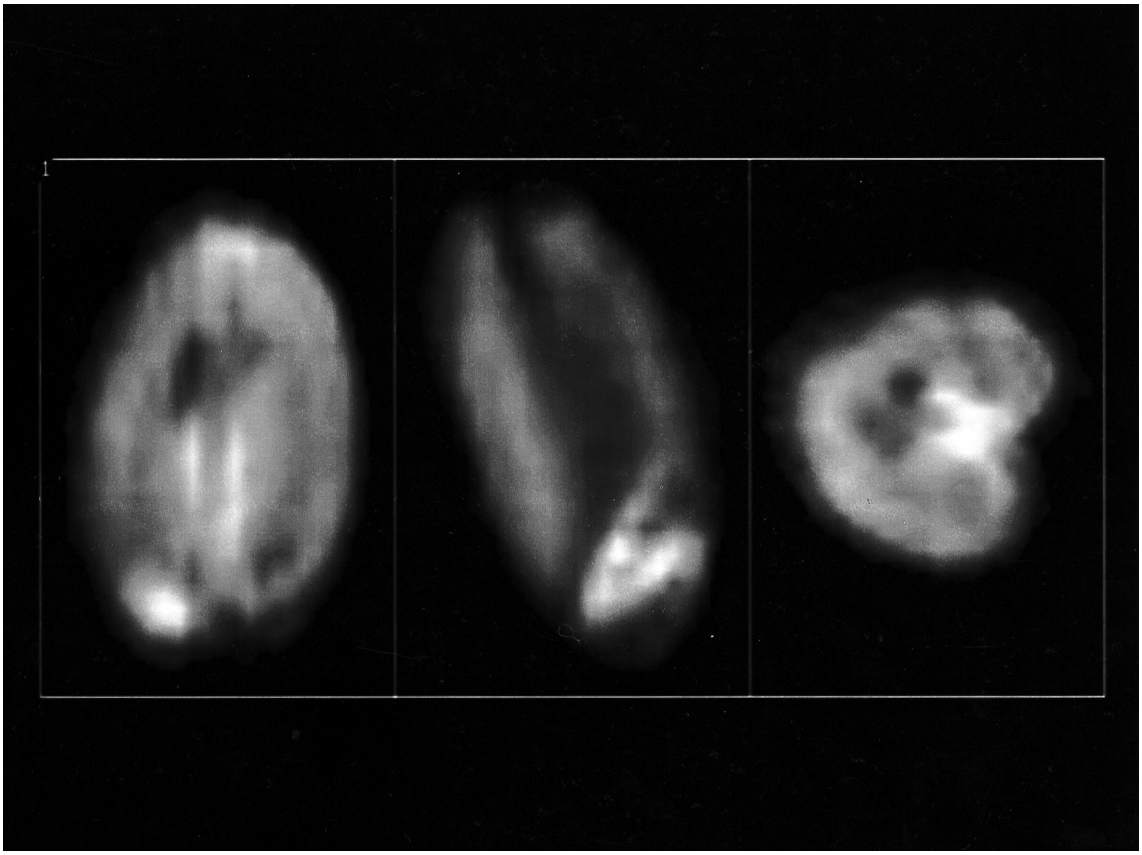

Figure 3 One central 2D proton image from each orthogonal view: Left image = slice 12 in dorsal-to-ventral view set, middle image = slice 11 in right-to-left view set, right image = slice 16 in distal-to-proximal view set.

After S, T_1, and T_2 of a voxel are measured, and experimental parameters T_E and T_R are set up, the proton density $N(H)$ of the voxel can be determined as

$$N(H) = S[1 - e^{-T_R/T_1}]^{-1}[e^{T_E/T_2}] \quad (3)$$

The magnetic gradient strengths in all three directions were $9{\cdot}8 \times 10^{-2}$ Tesla/m. The total number of projections was 3542 with the number of data points per projection being 128. The sequence delay time between two projections was 500 ms and T_E was 2·66 ms. The data acquistion time for each scan was 29·5 min. Because of the solid state of low-moisture wheat, eight scans were acquired for each image to increase the signal-to-noise ratio. The total time required to acquire each 3D image was 3 h 56 min. The temperature of the sample chamber during the experiment was controlled by circulating room temperature air (20°C) in the probe. The field of view was a sphere with 6 mm radius. This parameter set resulted in an average isotropic spatial resolution of $(94\ \mu m)^3$.

To simplify image processing, the endosperm was assumed uniform, thus all endosperm voxels were considered to have a constant relaxation time. With this assumption, the MR signal within regions of the endosperm becomes proportional to proton density $N(H)$, and hence proportional to the concentration of moisture or oil: the higher the moisture content, the brighter the image.

RESULTS AND DISCUSSION

A 3D image of a wheat grain is shown as a series of 2D contiguous slices in three orthogonal directions. The planes (**dorsal** = closest to dorsal surface; **ventral** = closest to ventral surface, **right** or **left** = closest to respective side; **distal** = closest to distal end, **proximal** = closest to proximal end) that define the orientation of the slices are shown in Figure 1. The T_1 and T_2 of the wheat grain were measured as 100 ms and 1.99 ms, respectively. Hence, the experimental parameters resulted in a

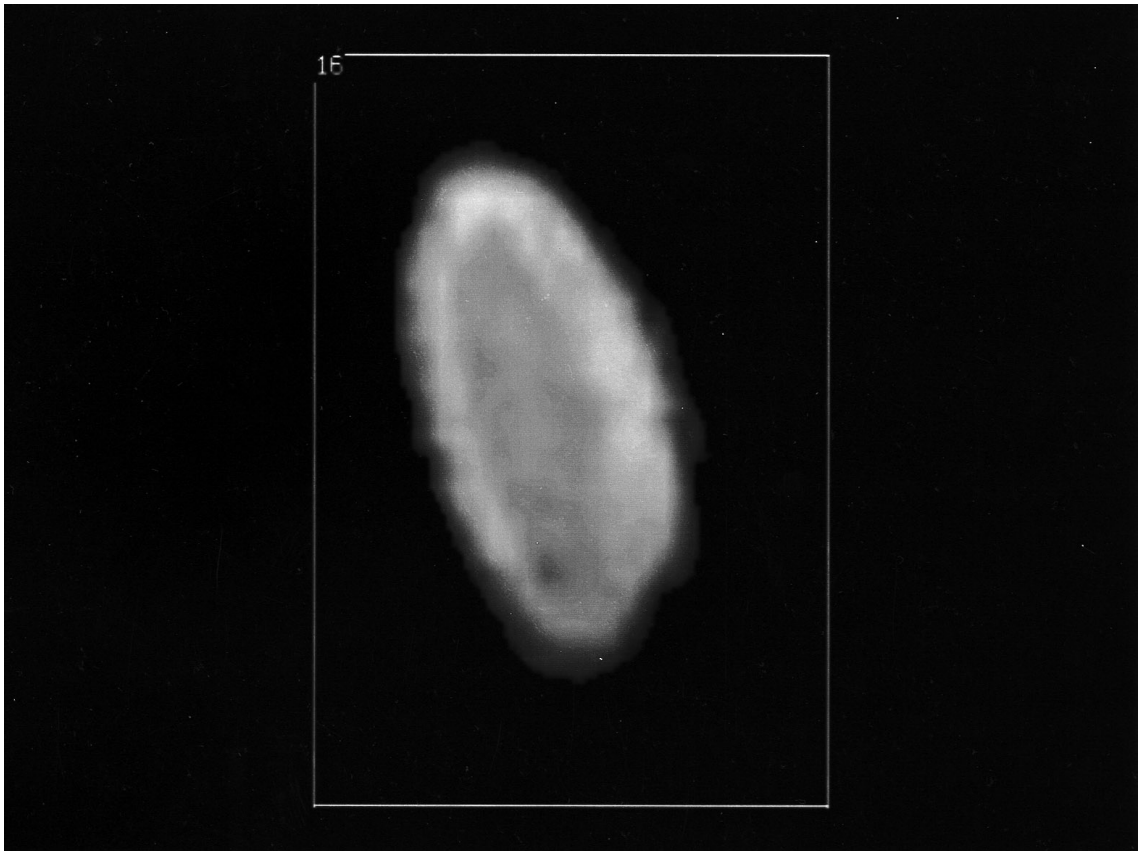

Figure 4 Two-dimensional proton image of wheat grain endosperm (slice 16 of right-to-left view set).

T_2-weighted image. Because the T_2 of the endosperm was considered constant, the T_2 factor only reduced image signal intensity by a constant [$\exp(-T_E/T_2) = 0{\cdot}2645$]. Therefore, the image intensity represented the proton density in the endosperm, which was proportional to the moisture distribution.

Figure 2(a) shows the dorsal-to-ventral views of the grain. The dark boundary of the images is the pericarp. The very bright irregularly shaped spot at the bottom of slices 1 through 12 is the germ. In slices 11 through 19, the white vertical lines near midspan are likely surface condensation on the epidermis within the crease region. The remaining region, shown as grey and within the pericarp but outside the germ and crease, is the endosperm. The moisture distribution in the endosperm was relatively uniform in slices 3 through 5. From slice 6 through slice 21, the dark region in the centre and the bright ring inside the pericarp indicate that the moisture was lower in the centre than in the outer region.

In the right-to-left views [Fig. 2(b)], the bright spot at the bottom (slices 4–13) is the image of the germ. The dark vertical band in the centre of image slices 7 through 14 represents the crease. Varying moisture level is evident in the right slices (4–6) and the left slices (15–20). Compared to the dorsal-to-ventral views, the moisture distribution was more uniform, though there was still variation in the endosperm. The moisture was higher near the periphery and lower in the interior (slices 5, 6, and 15–17).

From the distal-to-proximal views [Fig. 2(c)], the wide, bright area in the left region of slices 21 through 33 is the germ. The white spots in the right central region of slices 6 through 26 are attributed to the surface condensation on the epidermis within the crease region. Ring-like higher moisture distribution areas under the pericarp are evident in slices 9 through 23. Inside the ring, though still within the endosperm, the darker appearance of the image suggests a lower water concentration than in the ring itself.

Figure 3 displays one central 2D image in each of the three orthogonal directions (slice 12 in the dorsal-to-ventral view, slice 11 in the right-to-left view, and slice 16 in the distal-to-proximal view). From the pericarp to the centre of the grain, the moisture content gradually increased to its highest value, then decreased. To quantify moisture variation, a slice from the right-to-left view [slice 16, Fig. 2(b)] is enlarged in Figure 4. This slice encompasses only the endosperm. By application of Equation 3 and the assumption of a constant dry weight density throughout the endosperm, the localised moisture contents of portions within this region were calculated. The average moisture content of this high moisture ring was 14% wb with a variation of 13 to 16·4% wb. Similarly, in the central region of the grain, the moisture content was significantly lower and more uniform than the ring region. For this region, the lowest moisture content was 7·3% wb and the highest was 13% wb with an average moisture content of 11·2% wb.

SUMMARY AND CONCLUSION

A three-dimensional microscopic MRI with 3DPR technique was developed to measure the moisture distribution in a single mature wheat grain at a moisture content typical of storage conditions (*c.* 12% wb). A custom-designed RF coil and carefully selected MRI parameters were essential for imaging solid state low-moisture wheat grains. The isotropic spatial resolution of the images was $94 \times 94 \times 94\,\mu m^3$. Variations in endosperm moisture concentration (estimated range 7·3–16·4% wb) were revealed. Thus, non-destructive measurement of moisture within wheat grains is achievable by this form of MRI analysis.

Acknowledgement

This research was supported in part by USDA NRICGP grant 95-37500-1927.

REFERENCES

1. Friesen, T.L., Brusewitz, G.H. and Lowery, R.L. An acoustic method of measuring moisture content in grain. *Journal of Agricultural Engineering Research* **39** (1988) 49–56.
2. Zhang, X. and Brusewitz, G.H. Grain moisture measurement by microwave heating. *Transactions of the ASAE* **34** (1991) 246–250.
3. Miller, B.S., Lee, M.S., Hughes, J.W. and Pomeranz, Y. Measuring high moisture content of cereal grains by pulsed nuclear magnetic resonance. *Cereal Chemistry* **57** (1980) 126–129.
4. Morley, J.H., Fletcher, P.D. and Morgan, A.G. The estimation of moisture in whole grain wheat and barley nuclear magnetic resonance spectroscopy. *Journal of the National Institute of Agricultural Botany* **16** (1984) 437–442.
5. Brusewitz, G.H. and Stone, M.L. Wheat moisture by NMR. *Transactions of the ASAE* **30** (1987) 858–862.
6. Jenner, C.F., Xia, Y., Eccles, C.D. and Callaghan, P.T. Circulation of water within wheat grain revealed by nuclear magnetic resonance micro-imaging. *Nature* **336** (1988) 399–402.
7. Eccles, C.D., Callaghan, P.T. and Jenner, C.F. Measurement of the self-diffusion coefficient of water as a function of position in wheat grain using nuclear magnetic resonance imaging. *Biophysical Journal* **53** (1988) 77–81.
8. Brunner, P. and Ernst, R.R. Sensitivity in performance time in NMR imaging. *Journal of Magnetic Resonance* **33** (1979) 83–106.
9. Crooks, L.E. Selective irradiation line scan techniques of NMR imaging. *IEEE Transactions of Nuclear Science* **NS-27** (1980) 1239–1244.
10. Lauterbur, P.C. Image formation by induced local interactions: examples employing nuclear magnetic resonance. *Nature* **242** (1973) 190–191.
11. Lauterbur, P.C. Magnetic resonance zeugmatography. *Pure and Applied Chemistry* **40** (1974) 149–157.
12. Lauterbur, P.C. Spatially-resolved studies of whole tissues, organs, and organisms by NMR zeugmatography. In 'NMR in Biology', (R.A. Dwek, I.D. Campbell, R.E. Richards and R.J.P. Williams, eds) Academic Press, London (1977) pp 209–218.
13. Lauterbur, P.C. Medical imaging by nuclear magnetic resonance zeugmatography. *IEEE Transactions of Nuclear Science* **NS-26** (1979) 2808–2811.
14. Lauterbur, P.C., Kramer, D.M., House, W.V. Jr. and Chen, C.N. Zeugmatographic high resolution nuclear magnetic resonance spectroscopy. Image of chemical inhomogeneity within macroscopic objects. *Journal of the American Chemistry Society* **97** (1975) 6866–6868.
15. Mansfield, P. and Morris, P.G. 1982. NMR imaging in biomedicine. Supplement 2: Advances in Magnetic Resonance. Academic Press. New York (1982).
16. Zeng, X.S., Ruan, R.R., Fulcher, R.G. and Chen, P. Evaluation of soybean seedcoat cracking during drying: Part II. Using MRI. *Drying Technology* **14** (1996) 1595–1623.
17. Song, H.P., Litchfield, J.B. and Morris, H.D. Three-dimensional microscopic MRI of maize kernels during drying. *Journal of Agricultural Engineering Research* **53** (1992) 51–69.
18. Song, H. and Litchfield, J.B. 3D MR microscopy of foods during drying. In 'Food Dehydration', (G.V. Barbosa-Canovas and M.R. Okos, eds) AIChE, New York (1993) pp 55–71.
19. Song, H.P. and Litchfield, J.B. Measurement of stress cracking in maize kernels by magnetic resonance imaging. *Journal of Agricultural Engineering Research* **57** (1994) 109–118.
20. Song, H.P., Delwiche, S.R. and Line, M.J. Non-invasive measurement of moisture distribution in individual wheat kernels by magnetic resonance imaging. In 'SPIE Proceedings' (G.E. Meyer and J.A. DeShazer, eds) SPIE, Bellingham, WA **2345** (1994) pp 414–422.
21. Hahn, E.L. Spin echoes. *Physics Review* **80** (1950) 580–594.